Sugar-Integrated Gelators of Organic Solvents—Their Remarkable Diversity in Gelation Ability and Aggregate Structure

Kenji Yoza,[a] Natsuki Amanokura,[a] Yoshiyuki Ono,[a] Tetsuyuki Akao,[b] Hideyuki Shinmori,[c] Masayuki Takeuchi,[c] Seiji Shinkai,*[a] and David N. Reinhoudt[d]

Abstract: Five 1-*O*-methyl-4,6-*O*-benzylidene derivatives of the monosaccharides D-glucose, D-galactose, and D-mannose were synthesized. The β-isomer of the D-glucose derivative was sparingly soluble in most organic solvents, whereas the α-isomer of the D-mannose derivative was soluble in many organic solvents. The α-isomer of the D-glucose derivative and the α- and β-isomers of the D-galactose derivative acted as versatile gelators of various organic solvents; this indicates that saccharides are useful as potential templates for the molecular design of chiral gelators. In particular, the two D-galactose-based gelators behaved as "excellent gelators". It is very surprising that a change in the configuration of only one carbon atom results in such a drastic change in the solubility and the gelation properties. The possible relationship between the saccharide structure and the gelation properties is discussed on the basis of FT-IR and ^{1}H NMR spectroscopic data, differential scanning calorimetric (DSC) measurements, scanning electron microscopy (SEM) observations, and computational studies. FT-IR spectroscopy showed that the gelation properties are related to the formation of "moderate" intermolecular hydrogen bonds. The SEM observations showed that the gelators can form various fibrous structures (straight, puckered, and helical). The present study shows that this saccharide family is a potential combinatorial library of organic gelators and more generally, of molecular assembly systems.

Keywords: hydrogen bonds · molecular assembly · organic gels · saccharides · sol–gel processes · sugars · supramolecular chemistry

Introduction

The development of new gelators of organic solvents has recently received much attention. They not only gelatinize various organic solvents but also create novel networks with fibrous superstructures that can be characterized by SEM pictures of the xerogels.[1–11] The gelators can be classified into two categories according to the difference in the driving force for molecular aggregation: hydrogen-bond-based gelators and nonhydrogen-bond-based gelators. Typical examples of the former group are aliphatic amide derivatives,[1–4] and of the latter group, cholesterol derivatives.[6–9] The superstructures observed as fibrous aggregates in the organic gels of aliphatic amide derivatives satisfy the complementarity for intermolecular hydrogen-bond interactions.[5–9] This observation stimulated us to use saccharides as a hydrogen-bond-forming segment in gelators, because one can then easily introduce a variety of hydrogen-bond-forming, chiral segments into the gelators by appropriate selection from a saccharide library. It is expected, therefore, that many sugar-integrated gelators can be readily designed by substituting this segment only, leading eventually to new chiral gelators. However, literature examples of saccharide-containing gelators are very limited in spite of their high potential.[8, 12] In this paper, we report on the syntheses of the α-isomers of the glucose derivative **1a**, the galactose derivative **2a**, and the mannose derivative **3a** and the β-isomers of the glucose derivative **1b** and the galactose derivative **2b** and their gelation abilities. We found that the gelation properties (e.g., gel stability, gel fiber superstructure, solvent dependence, etc.) are clearly related to the saccharide structure.[13]

[a] Prof. S. Shinkai, Dr. K. Yoza, N. Amanokura, Y. Ono
Chemotransfiguration Project
Japan Science and Technology Corporation
Aikawa, Kurume, Fukuoka 839–0861 (Japan)
Fax: (+81) 942 39 9012
e-mail: seijitcm@mbox.nc.kyushu-u.ac.jp

[b] Dr. T. Akao
Biotechnology and Food Research Institute
Fukuoka Industrial Technology Center
Aikawa, Kurume, Fukuoka 839-0861 (Japan)

[c] Dr. H. Shinmori, Dr. M. Takeuchi
Department of Chemistry and Biochemistry
Graduate School of Engineering
Kyushu University, Hakozaki, Higashi-ku, Fukuoka 812-8581 (Japan)

[d] Prof. D. N. Reinhoudt
Chemotransfiguration Project, Faculty of Chemical Technology
University of Twente, 7500 AE Enschede (The Netherlands)

© WILEY-VCH Verlag GmbH, D-69451 Weinheim, 1999
0947-6539/99/0509-2722 $ 17.50+.50/0

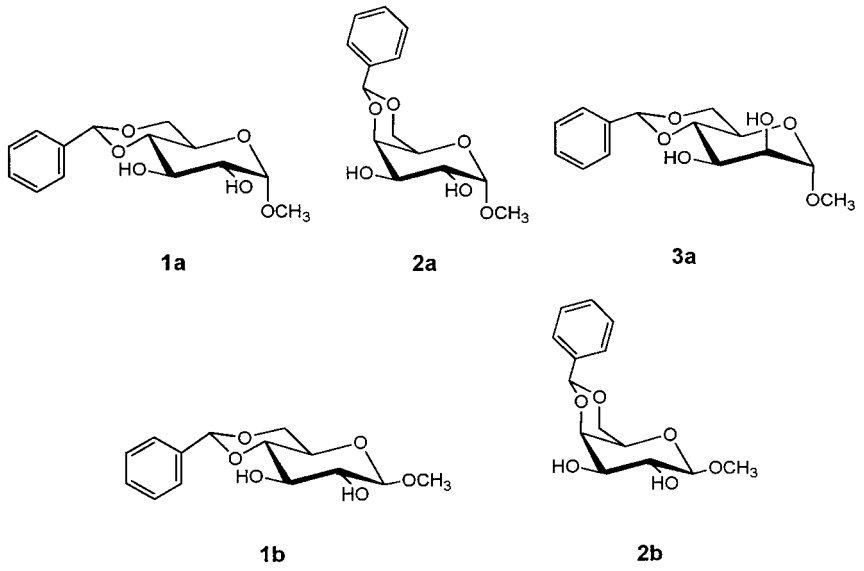

Results and Discussion

Gelation test for various organic solvents: The synthesis of **1a** has already been reported.[14] The other gelators were synthesized in a similar manner by treatment of the corresponding saccharides with benzaldehyde and $ZnCl_2$. The products were identified by ^1H NMR and IR spectroscopy and elemental analyses (see the Experimental Section).

The gelation test was carried out as follows: the gelator (3.0 mg) was mixed with solvent (0.10 mL) in a septum-capped test tube, and the mixture was heated until the solid dissolved. The solution was cooled to 25 °C and left for 1 h. A "G" in Table 1 denotes that a gel was formed at this stage. Some solutions gelled at a gelator concentration below 1.0% (wt/vol) and are designated "G*" in Table 1. Solvents in Group I are those which were gelatinized by some gelators. Solvents in Group II are those in which all the gelators were either too soluble or precipitated.[15] From examination of Table 1, several interesting points can be inferred as characteristic of sugar-integrated gelators. Firstly, among the three α-isomers, **2a** is the best gelator of many organic solvents. Secondly, comparison of the gelation ability for *n*-hexane, cyclohexane, and Group II solvents reveals that **1a** is more cohesive and tends to form a precipitate, whereas **3a** is more soluble than the other two gelators and is frequently unable to coagulate in solution. Thirdly, the β-isomer of galactose derivative **2b** also acts as an excellent gelator, comparable with **2a**. Finally, the solubility of the β-isomer **1b** is generally inferior to that of the α-isomer **1a** as indicated by the numerous "P" (P = precipitation) entries for **1b** and the "S" (S = solution) entriees for **1A**.

As seen from the saccharide structures illustrated above, **1a**, **2a**, and **3a** are epimers that differ only in the carbon configuration at either C-2 or C-4, whereas **1a**–**1b** and **2a**–**2b** are anomers with one different carbon configuration at C-1. It is surprising that a difference in the carbon configuration results in such a marked difference in the solubility or gelation properties. The possible rationale for the structure-gelation relationship is discussed below.

Concentration dependence: In Figure 1, the sol–gel phase transition temperatures (T_{gel}) of **1a**, **2a**, **3a**, and **2b** in toluene and diphenyl ether are plotted against the gelator concentration in order to compare their gelation properties. Figure 1 shows that in both solvents the T_{gel} values at the same gelator concentration always appear in the order **2a** > **1a** > **3a** for the α-isomers, whereas the T_{gel} values for **2b** are always higher than those for **2a**. Figure 2 shows similar plots in benzene, carbon tetrachloride, and water. Again, a similar trend is observed here; both in benzene and in carbon tetrachloride, the T_{gel} values for **2a** are higher than those for **1a**. Judging from the foregoing gelation test, one may conclude that the cohesive nature of the five gelators decreases in the order **1b** > **2b** > **2a** > **1a** > **3a**.

Table 1. Organic solvents tested for gelation by **1a, 1b, 2a, 2b**, and **3a**.[a]

	1a	**1b**	**2a**	**2b**	**3a**
Group I					
n-hexane	G*	P	G*	G*	G*
n-heptane	P	P	G*	G*	G*
n-octane	G*	P	G*	G*	G*
cyclohexane	P	P	G*	G*	G*
methylcyclohexane	G*	P	G*	G*	G*
benzene	G	P	G*	G*	P
toluene	G*	P	G*	G*	G*
p-xylene	G*	P	G*	G*	G*
nitrobenzene	S	P	S	Gp	S
carbon tetrachloride	G*	P	G*	G*	P
carbon disulfide	P	G	G*	G*	G*
diethyl ether	G	P	G*	P	P
diphenyl ether	G*	G	G*	G*	G
ethyl formate	S	P	P	Gp	S
methyl acetate	S	P	S	Gp	S
n-octanol	S	P	G	G	S
triethylamine	S	P	G	G	S
triethylsilane	P	P	Gp	G	G*
tetraethoxysilane	P	P	G*	P	P
water	P	P	S	S	G
Group II					
1,2-dichloroethane	S	P	S	S	S
dichloromethane	S	P	S	S	S
chloroform	S	P	S	S	S
ethyl acetate	S	P	P	S	S
ethyl malonate	S	P	S	S	S
acetone	S	P	S	S	S
methyl ethyl ketone	S	P	S	S	S
acetonitrile	S	P	S	S	S
ethanol	S	P	S	S	S
n-propanol	P	P	P	P	S
n-butanol	P	P	S	P	S
hexanoic acid	S	P	P	P	S
acetic anhydride	S	P	S	S	S
glycerol	S	P	S	S	S

[a] G = gel; G* = gelated even under 1.0 wt/vol%; Gp = partial gel; P = precipitation; S = solution.

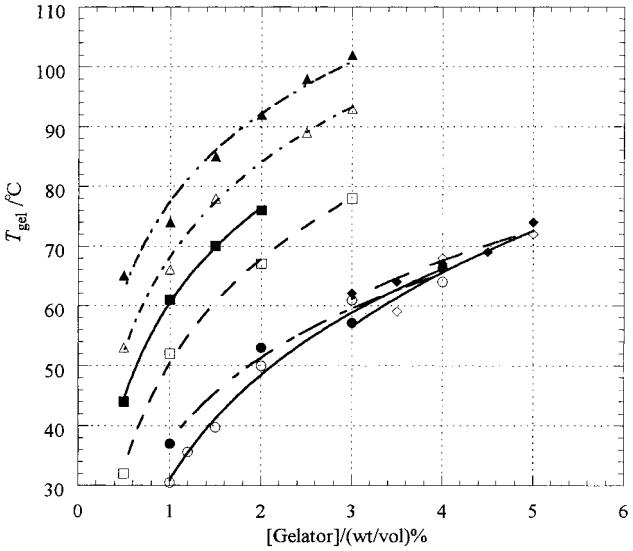

Figure 1. Plots of T_{gel} against gelator concentration in toluene and diphenyl ether: **1a**/diphenyl ether (○), **1a**/toluene (●), **2a**/diphenyl ether (□), **2a**/toluene (■), **3a**/diphenyl ether (◇), **3a**/toluene (◆), **2b**/diphenyl ether (△), **2b**/toluene (▲).

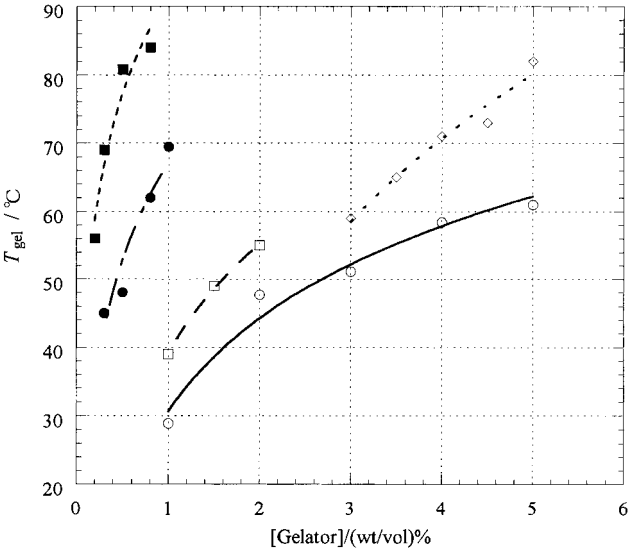

Figure 2. Plots of T_{gel} against gelator concentration in benzene, carbon tetrachloride, and water: **1a**/benzene (○), **1a**/CCl_4 (●), **2a**/benzene (□), **2a**/CCl_4 (■), **3a**/water (◇).

Previously, we derived [Eq. (1)] from a Schrader's relation frequently used for the dissolution of solid compounds in organic solvents.[7] ΔH can be determined from the slope of a

$$\log[\text{gelator}] = -\frac{\Delta H}{2.303\,R} \times \frac{1}{T_{gel}} + \text{constant} \quad (1)$$

plot of log[gelator] (with the gelator concentration given in mol − 1 dm^{-3}) against T_{gel}^{-1}. It is known that the ΔH values are comparable with or slightly larger than the latent heat of fusion ΔH_f values determined from DSC measurements at the melting point of the solid.[7] This might indicate that the ΔH values reflect the heat released at the sol–gel phase transition temperature. This implies albeit indirectly that the gelator fibers formed in organic solvents are not so solvated with solvent molecules.[7, 16]

However, we do not consider that this corresponds with a "perfect" gel-monomer transition. For example, we observed the sol–gel phase transition under an optical microscope. Although the mobility of the solution system was drastically increased above the T_{gel}, small aggregate particles still exist. One may consider, therefore, that some gelators aggregate even in the solution phase.

As shown in Figure 3, plots of log[gelator] against T_{gel}^{-1} afforded straight lines with γ(correlation coefficient) > 0.97. The ΔH values estimated on the basis of Equation 1 are

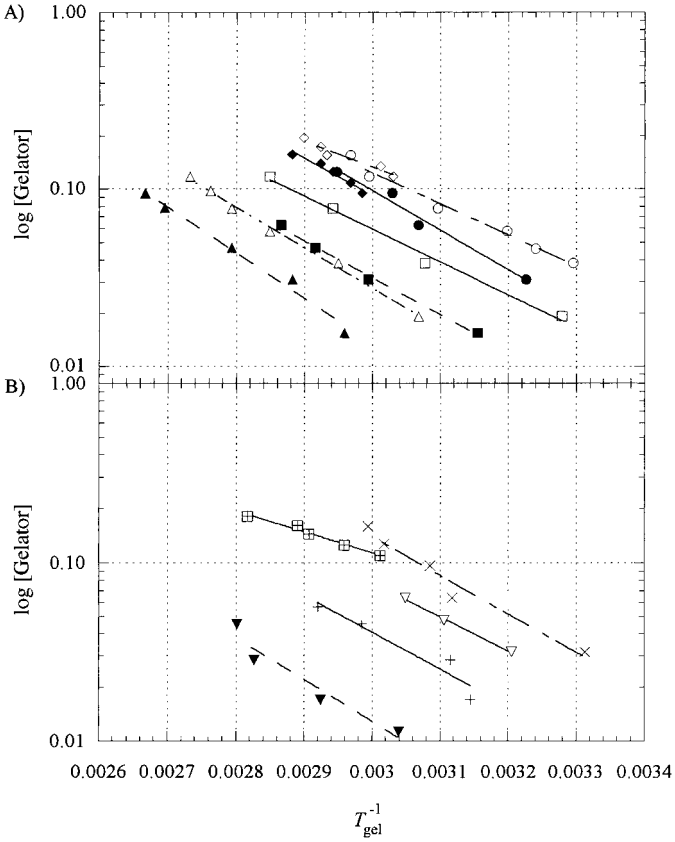

Figure 3. Plots of log[gelator] (gelator concentration in mol dm^{-3}) against T_{gel}^{-1}. A) (toluene and diphenyl ether system): **1a**/toluene (●), **1a**/diphenyl ether (○), **2a**/toluene (■), **2a**/diphenyl ether (□), **3a**/toluene (◆), **3a**/diphenyl ether (◇), **2b**/toluene (▲), **2b**/diphenyl ether (△). B) (benzene, CCl_4, and water system); **1a**/benzene (×), **1a**/CCl_4 (+), **2a**/benzene (▽), **2a**/CCl_4 (▼), **3a**/water (⊡).

summarized in Table 2. The ΔH_f values at the melting points as determined by DSC mesurements were 23, 27, 22, 25, and 26 kJ mol^{-1} for **1a**, **2a**, **3a**, **1b**, and **2b**, respectively. Although

Table 2. ΔH obtained from [gelator] *vs.* T_{gel} plots and ΔH_f at the melting point obtained from DSC measurements.

	ΔH kJ mol^{-1}					ΔH_f kJ mol^{-1}
	Toluene	Diphenyl ether	Benzene	CCl_4	Water	
1a	43	33	42	40	ppt[a]	23
2a	40	35	37	45	S[b]	27
3a	41	28[c]	ppt[a]	ppt[a]	22	22
1b	ppt[a]	–	ppt[a]	ppt[a]	ppt[a]	25
2b	49	44	–	–	S[b]	26

[a] Gelators were precipitated from these solvents. [b] Gelator were soluble in these solvents. [c] The correlation coefficient in Figure 3 is 0.97.

© WILEY-VCH Verlag GmbH, D-69451 Weinheim, 1999
0947-6539/99/0509-2724 $ 17.50+.50/0 *Chem. Eur. J.* **1999**, *5*, No. 9

the ΔH_f values decrease in the order **2a** > **2b** > **1b** > **1a** > **3a**, the differences are relatively small. As described later under the FT-IR measurements, the ν_{OH} peak assignable to the free OH group could not be found for the solid gelator samples. This means that in the solid state all the OH groups in these gelators form either intramolecular or intermolecular hydrogen bonds. This situation should result in averaged ΔH_f values. It is interesting to note, however, that the excellent gelators **2a** and **2b** have relatively large ΔH_f values, whereas the very soluble gelator **3a** has a relatively small ΔH_f value.[17] Table 2 also shows that the ΔH values are generally larger than the ΔH_f values and have characteristic solvent dependence. Firstly, ΔH values in the hydrocarbon solvents, toluene and benzene, are generally larger than in oxygen-containing solvents (diphenyl ether). This implies that diphenyl ether acts as a hydrogen-bond acceptor and weakens the network formation based on the intermolecular hydrogen-bond interaction. Secondly, **3a**–diphenyl ether and **3a**–water systems have small ΔH values, 28 and 22 kJ mol^{-1} respectively. Gelator **3a** is relatively soluble in these solvents, and the gel is obtained only in the high concentration region (see Figures 1 and 2). Thus, a small ΔH value is attributed to the affinity (or partial dissolution) of the gelator for solvent molecules. Clearly water is not a favorable solvent for gelation with sugar-integrated gelators that utilize the intermolecular hydrogen-bond interaction for network formation. However, it is rather surprising that water could be gelatinized by **3a**. Thirdly, **2b** which is the best of the five gelators tested herein affords the largest ΔH values. This finding indicates that the stable gel formation with high T_{gel} is related to the formation of stable, intermolecular hydrogen bonds, as reflected in the large ΔH values.

The order of the ΔH values is solvent dependent. Generally speaking however, the order is **2b** > **1a** ≈ **2a** > **3a**. This order is roughly coincident with the ΔH_f values and also supports the view that the gel fibers are not so solvated with solvent molecules, but are composed of aggregates of solid-like particles.

Intermolecular hydrogen-bond interactions as detected by FT-IR spectroscopy: In the FT-IR spectra, the ν_{OH} peak of the free OH group (at around 3600 cm^{-1}) was not found for solid samples of the five gelators. This indicates that all the OH groups form either intermolecular or intramolecular hydrogen bonds. On the other hand, the gel solutions exhibited two peaks at 3220–3475 and 3573–3588 cm^{-1} in the ν_{OH} region, which could be assigned to hydrogen-bonded OH and free OH groups, respectively. Typical FT-IR spectra are shown in Figure 4. The **1a**–toluene system shows two broad peaks around 3328 and 3389 cm^{-1} in addition to a ν_{OH} peak at 3577 cm^{-1} for free OH groups. The **1b**–toluene and **3a**–toluene systems exhibit similar broad ν_{OH} peaks for the hydrogen-bonded OH groups. The appearance of the broad peaks suggests that the hydrogen-bonded network in these systems is relatively disordered. On the other hand, in the **2a**–toluene system there are three sharp peaks at 3314, 3429, and 3475 cm^{-1} in addition to a peak at 3573 cm^{-1} for free OH groups. The **2b**–toluene system was similar to the **2a**–toluene system, in giving rise to three sharp ν_{OH} peaks, Table 3.

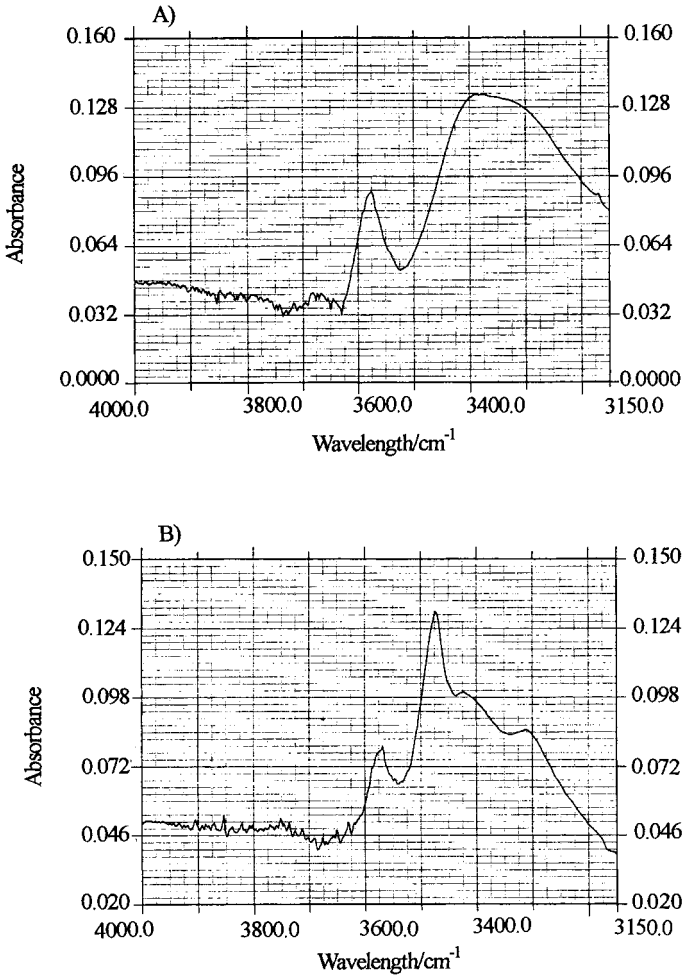

Figure 4. FT-IR spectra at 25 °C of: A) **1a**/toluene system (0.80 % (wt/vol)) and B) **2a**/toluene system (0.28 % (wt/vol)).

Table 3. ν_{OH} bands (cm^{-1}) of the gels prepared from the toluene solutions.

	Concentration [(wt/vol) %]	Free OH [cm^{-1}][a]	Hydrogen-bonded OH [cm^{-1}][a]
1a	0.60	3577(sh)	3328(br), 3389(br)
2a	0.26	3573(sh)	3314(sh), 3429(sh), 3475(sh)
3a	0.60	3577(sh)	3235(br), 3350(br)
1b	0.40 (ppt)[b]	3577(sh)	3220(br), 3377(br)
2b	0.15	3588(sh)	3280(sh), 3373(sh), 3440(sh)

[a] sh = sharp peak; br = broad peak. [b] The sample is the solution containing the precipitate.

This might mean that the hydrogen-bond interaction in these systems is more ordered, with a high degree of complementartiy between the hydrogen-bond-forming OH groups. It is important to note that **2a** and **2b**, which show the three sharp ν_{OH} peaks, are excellent gelators. These findings lead us to conclude that in these systems the complementarity of the OH groups is the primary factor in controlling organic gel stability.

Figure 5 shows that the peak intensity ratio (R) of hydrogen-bonded OH to free OH abruptly increases at the sol–gel phase transition concentration. For excellent gelators such as **2a** and **2b**, the ν_{OH} peaks for hydrogen-bonded OH groups appear even at low gelator concentrations [ca. 0.1–0.2 % (wt/vol)], whereas those for **1a** and **3a** appear only at high gelator

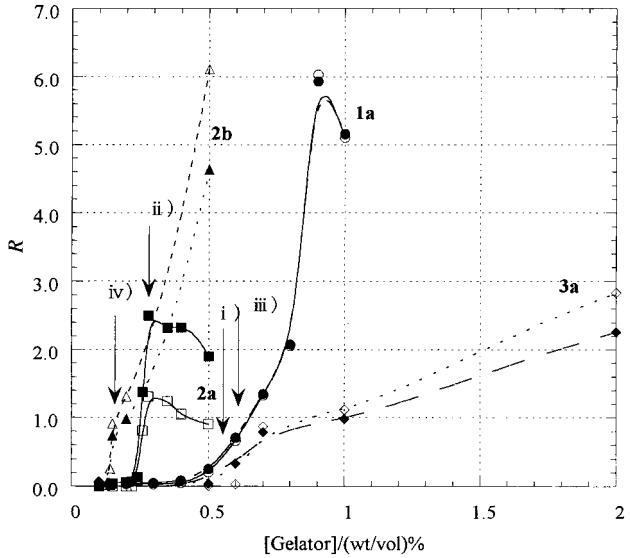

Figure 5. Plots of the peak intensity ratio R of hydrogen bonded to free OH groups as a function of gelator concentration in toluene at 20 °C. There are two major peaks for hydrogen-bonded OH groups; the filled points were obtained from the intensities at $\nu_{OH} = 3220-3314$ cm^{-1}, whereas the open points were obtained from those at $\nu_{OH} = 3350-3429$ cm^{-1}; (○,●) **1a**, (□,■) **2a**, (◇,◆) **3a**, and (△,▲) **2b**. The arrows indicate the sol–gel transition temperature of i) **1a**, ii) **2a**, iii) **3a**, and iv) **2b**.

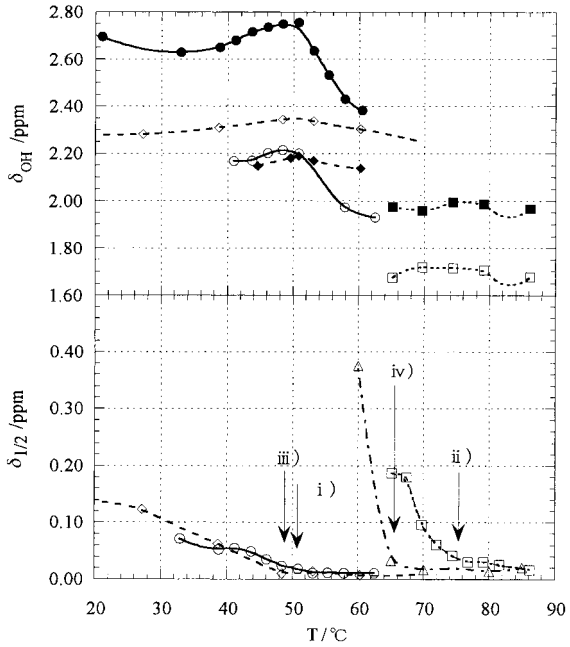

Figure 6. Plots of δ_{OH} the OH group chemical shift and $\delta_{1/2}$ the half-height peak width of the PhCH methine proton peak against temperature; [**1a**] = [**2a**] = [**3a**] = 2.0% (wt/vol) in [D_8]toluene. There are two peaks for the OH groups: (○,●) **1a**, (□,■) **2a**, (◇,◆) **3a**; $\delta_{1/2}$ (○) **1a**, (□) **2a**, (◇) **3a**, (△) **2b**. The arrows indicate the sol–gel transition temperature of i) **1a**, ii) **2a**, iii) **3a**, and iv) **2b**.

concentrations [ca. 0.5% (wt/vol)]. In particular, the value of R for **3a** increases very gradually with increasing **3a** concentration. This means that **3a** is very soluble in toluene and the gel fibers are created gradually under the disadvantageous condition by which an equilibrium of monomeric **3a** with aggregated **3a** favours monomeric **3a** . It is not yet clear what structural factor governs the magnitude of the R value. If this measure could be correlated with the complementarity of the intermolecular hydrogen bonds, **2b** would be expected to have one of the highest R values as in fact it does (Figure 5). However, **1a** is significantly inferior to **2a** in its gelation ability, but it has an R value comparable with **2a**. [18] It is likely therefore, that the R value reflects mainly the structure of the solid-like gel fibers, whereas the gelation ability is related not only to the fiber structure but also to the solubility of gelators or their affinity for solvent molecules. This difference may cause the disagreement between the gelation ability and the R value.

The foregoing FT-IR spectroscopic data consistently support the view that the gel network in the present system is primarily stabilized by intermolecular hydrogen bonding. Judging from the plots in Figure 5, the molecular coagulation tendency decreases in the order: **2b** > **2a** > **1a** > **3a**. This order coincides with that estimated from the gelation test (vide supra).

Temperature-dependent ^{1}H NMR spectra: It is to be expected that the molecular motion of gelators drastically changes at the sol–gel phase transition temperature T_{gel}. This change can be conveniently monitored by the line-broadening effect in the ^{1}H NMR spectrum. In fact, such a phenomenon has already been reported for a related gel system.[19] We have measured the ^{1}H NMR spectra of **1a**, **2a**, **3a** [each at 2.0% (wt/vol)], and **2b** [0.50% (wt/vol)] in [D_8]toluene at 25–83 °C. As shown in Figure 6, the half-height peak width $\delta_{1/2}$ of the PhCH methine proton is nearly constant above the T_{gel}, while it increases with falling temperature below the $T_{gel.}$ The results imply that the mobility of gelator molecules is significantly suppressed in the gel phase, whereas it is comparable with that of the homogeneous solution in the sol phase. On the other hand, plots of δ_{OH} (chemical shift of the OH groups) against temperature for **1a**, **2a**, and **3a** show that the chemical shifts have their maximum downfield values at the T_{gel}. In general, the formation of strong hydrogen bonds with OH groups induces a downfield shift of δ_{OH}.[20, 21] Hence, the hydrogen bonds with the OH groups are strengthened with lowering of the medium temperature from the sol phase to the T_{gel} region. This change is explicable in terms of intermolecular aggregation near the gel region. In contrast, it is difficult to explain why the hydrogen bonds are gradually weakened as the medium temperature falls in the gel phase. Presumably, in the T_{gel} region the formation of the "soft gel" is predominantly governed by the intermolecular hydrogen-bond interaction, but at temperatures much lower than T_{gel}, the formation of the crystal-like "hard gel" [7, 16] is governed not only by the intermolecular hydrogen-bond interaction but also by other intermolecular forces such as $\pi-\pi$ interactions, van der Waals interactions, etc.[10] In cases in which the latter forces cannot harmonize with the hydrogen-bond interaction because of steric mismatching, the hydrogen bonds may be weakened with decreasing medium temperature. In any event, it is clear that ^{1}H NMR spectroscopy is a potential tool for studying the formation of organic gels.

SEM observations of xerogels: In order to obtain visual insights into the aggregation mode, we have prepared dry samples of organic gel fibers for SEM studies.[22] Figure 7 (a

© WILEY-VCH Verlag GmbH, D-69451 Weinheim, 1999
0947-6539/99/0509-2726 $ 17.50+.50/0 *Chem. Eur. J.* **1999**, *5*, No. 9

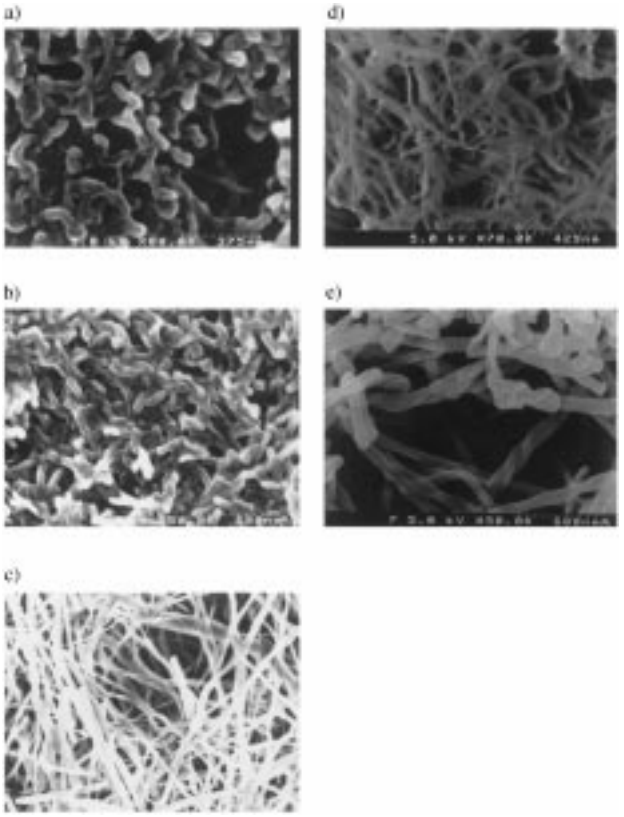

Figure 7. SEM pictures of **1a**, **2a**, **3a**, and **2b**: a) **1a** prepared from carbon tetrachloride [0.5% (wt/vol)], b) **2a** prepared from carbon tetrachloride [0.5% (wt/vol)], c) **3a** prepared from toluene [3.0% (wt/vol)], d) **2b** prepared from benzene [1.0% (wt/vol)], and e) **3a** prepared from water [3.0% (wt/vol)].

and b) shows typical pictures obtained from xerogels of **1a** or **2a** in carbon tetrachloride. It is clear that the gelators form a three-dimensional network with 50–200 nm puckered fibrils. On the other hand, the fibrils obtained from the gel of **3a** with toluene and of **2b** with benzene are more linear (Figure 7, c and d). Interestingly, the fibrils obtained from the aqueous gel of **3a** show a regular left-handed helical structure, Figure 7e. Presumably, in an aqueous system the balance between hydrogen-bond interaction and hydrophobic interaction is different from that in organic media. This problem is currently under investigation to clarify a possible relationship between the gelator structure and the aggregate morphology.

Computational studies: The above-mentioned results consistently support the view that the slight difference in the saccharide configuration is largely reflected by the solubility, the gelation ability, and the superstructure of the gel fibers. What is the origin of these differences? Although the gel fiber structure is not necessarily the same as that obtained from the single-crystal X-ray studies,[5] X-ray crystallography should give some useful information. Unfortunately, these gelators tend to grow as needles and single crystals suitable for X-ray analysis have not been isolated so far. Thus, in order to obtain some insight into the difference in the solubility (which is eventually related to the gelation ability), we undertook some computational studies with MM3. The energy-minimized structures in their C1 forms are illustrated in Figure 8.

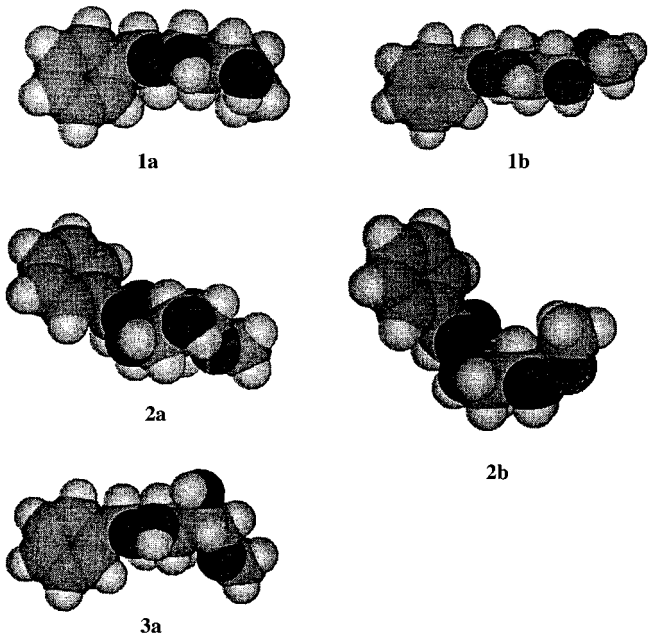

Figure 8. Energy-minimized structures of **1a**, **2a**, **3a**, **1b**, and **2b** in their C1 forms predicted on the basis of MM3 calculations.

It is known that the physical properties of certain gelators are affected by epimeric effects.[6b] In the present system, the solubility of **1b** is the lowest of the five saccharide-based gelators tested herein (Table 1). Two features of this compound are that the molecular structure is relatively "flat", because of the β-configuration of the 1-OMe group, and two unmodified OH groups occupy the sterically less crowded equatorial position. These steric characteristics should facilitate intermolecular aggregation, which occurs through the stacking of pyranose rings and hydrogen-bond interaction among the OH groups. In contrast, the solubility of **3a** is the highest of the five saccharide-based gelators tested here (Table 1). Two relevant features of this compound are that the molecular structure is L-configured, because of the α-configuration of the 1-OMe group, and one of the two unmodified OH groups occupies the sterically more crowded axial position. In fact, of the five gelators, only **3a** has an axial OH group. These steric characteristics should suppress the intermolecular aggregation tendency and eventually enhance the solubility. Gelator **1a**, which has an α-1-OMe group and two equatorial OH groups, has intermediate solubility and gelation properties between **1b** and **3a** (Table 1).

So why do **2a** and **2b**, prepared from D-galactose, possess such excellent gelation ability? Based on the above discussion, it is beyond doubt that the primary reason is related to their axial 4-OR substituent, which forces **2a** and **2b** to adopt an L-configuration. As seen in Figure 8, the pyranose rings are almost perpendicular to the benzene rings, an orientation that hinders intermolecular aggregation. But they have two equatorial OH groups which favor intermolecular aggregation. These two opposing effects within the same gelator molecule should create excellent gelation properties. As a principle for the molecular design of gelators, therefore, one may propose that they will produce a precipitate if the intermolecular aggregation forces are too strong, whereas the

gelators will be solubilized in solution if the intermolecular forces are too weak. In addition, galactose-based **2a** and **2b** have an additional structural characteristic that the other gelators do not possess. In cyclohexane derivatives the bulky substituent tends to occupy the equatorial position. This stereochemical requirement should also be valid for the pyranose ring. This is achieved by ring inversion of the C1 structure to the 1C structure, forcing the axial 1-OMe into an equatorial position. In **1a**, **1b**, and **3a**, however, both the 4-OR and 5-CH_2OR groups occupy an equatorial position, so that inversion to the 1C structure would force them into the *trans*-axial position. This process is unrealistic because the 4-OR and 5-CH_2OR groups form a 1,3-dioxane ring. In other words, the C1 structure in Figure 8 is the only possible conformation. In contrast, the 4-OR and 5-CH_2OR groups in **2a** and **2b** occupy the axial and equatorial positions, respectively. Hence inversion of the pyranose ring is possible to give structure 1C; in this conformation the 1-OMe group can move to the less crowded equatorial position (Figure 9).

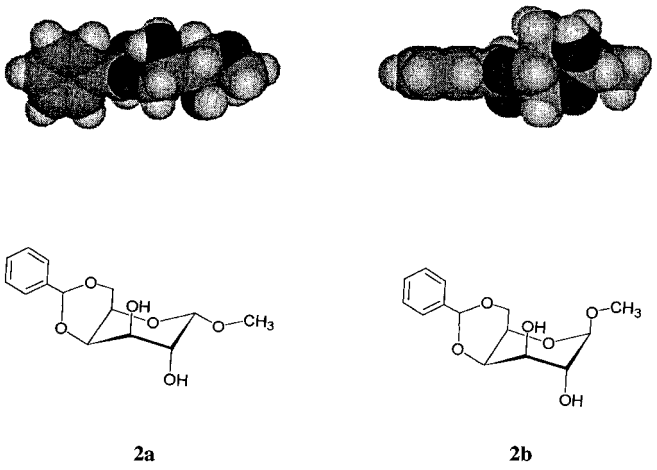

Figure 9. Energy-minimized structures of **2a** and **2b** in their 1C forms predicted on the basis of MM3 calculations.

This structural variation may improve the ability of **2a** and **2b** to form a complementary hydrogen-bond network in their aggregates and prevent precipitation or crystallization.[23] Judging from the three above-mentioned charactistics, the L-configuration, the presence of unique OH groups, and interconversion between the C1 and the 1C forms, we can conclude that D-galactose serves as the best template for designing excellent gelators of organic solvents.

Conclusions

The present study has demonstrated that saccharides serve as promising templates for the molecular design of new gelators with different gelation properties and different three-dimensional network structures. Surprisingly, we have found that the gelation ability is drastically changed by a slight change in the saccharide configuration. The gelation ability is predictable to some extent from physical parameters, such as ν_{OH} from FT-IR, δ_{OH} from ^{1}H NMR, ΔH_f from DSC, and solubility in organic solvents. In the present system, these parameters tend to appear in the order: **1b** (too cohesive) > **1a**, **2a**, **2b** (moderately cohesive; suitable for gelation) > **3b** (less cohesive; too soluble). We believe that such a convenient synthetic route and remarkable diversity in the gelation ability and the gel fiber structure (including the creation of the helical structure) can hardly be attained in a more simple fashion than with saccharide templates. More concisely, the present paper has shown the high potential of saccharide-based molecules for gel formation. We believe that the saccharide library provided by nature can be applied further, in particular to the design of molecular assemblies, such as macrocycles, DNA mimics, monolayers, bilayer membranes, liquid crystals, etc.

Experimental Section

Methyl-4,6-*O*-benzylidene-*α*-D-glucopyranoside (1a): Compound **1a** was synthesized according to the method described in the literature.[14] A mixture of benzaldehyde (5.0 mL, 49.5 mmol) and methyl-*α*-D-glucopyranoside (2.0 g, 10.3 mmol) was stirred with zinc chloride (1.50 g, 11.0 mmol) under a nitrogen atmosphere. The reaction was continued at room temperature for 6 h. After the reaction mixture was added to water (50 mL), the product thus precipitated was collected by filtration. The precipitate was washed with water and *n*-hexane and then reprecipitated by chloroform/*n*-hexane: yield (2.27 g, 78%) (calculated from methyl-*α*-D-glucopyranoside). M.p. 165.4–166.8 °C; ^{1}H NMR (300 MHz, $CDCl_3$, 25 °C, TMS): $\delta = 2.46$ (br s, 1H; OH), 2.95 (br s, 1H; OH), 3.45 (s, 3H; OMe), 3.48–4.31 (m, 6H; sugar–CH (H2–6)), 4.77 (d, 1H; sugar–H (H1)), 5.52 (s, 1H; Ph–CH), 7.35–7.38 (m, 3H; *m*,*p*-Ph–H), 7.45–7.51 (m, 2H; *o*-Ph–H); IR (KBr): $\tilde{\nu} = 3650-3100$ (OH), 1030 cm^{-1} (C–O–C); $C_{14}H_{18}O_6$ (282.3): calcd C 59.57, H 6.43; found C 58.21, H 6.55; $C_{14}H_{18}O_6 \cdot 0.4H_2O$ requires C 58.07, H 6.56.

Methyl-4,6-*O*-benzylidene-*α*-D-galactopyranoside (2a): Compound **2a** was synthesized by means of a method similar to that used for **1a**:[13] yield (1.12 g, 39%) (calculated from methyl-*α*-D-galactopyranoside). M.p. 168.9–170.5 °C; ^{1}H NMR (300 MHz, $CDCl_3$, 25 °C, TMS): $\delta = 2.30$ (br s, 1H; OH), 2.52 (br s, 1H; OH), 3.46 (s, 3H; OMe), 3.70–4.31 (m, 6H; sugar–CH (H2–6)), 4.93 (d, 1H; sugar–H (H1)), 5.55 (s, 1H; Ph–CH), 7.36–7.38 (m, 3H; *m*,*p*-Ph–CH), 7.48–7.52 (m, 2H; *o*-Ph–H); IR (KBr): $\tilde{\nu} = 3640-3100$ (OH), 1030 cm^{-1} (C–O–C); $C_{14}H_{18}O_6$ (282.3): calcd C 59.57, H 6.43; found C 58.09, H 6.35; $C_{14}H_{18}O_6 \cdot 0.4H_2O$ requires C 58.07, H 6.56.

Methyl-4,6-*O*-benzylidene-*α*-D-mannopyranoside (3a): Compound **3a** was synthesized by means of a method similar to that used for **1a** and was purified by column chromatography (silica gel, $CHCl_3$/MeOH 30:1 (v/v); $R_f = 0.14$). This product was reprecipitated by chloroform/*n*-hexane: yield (190 mg, 7%) (calculated from methyl-*α*-D-mannopyranoside). M.p. 131.1–133.7 °C; ^{1}H NMR (300 MHz, $CDCl_3$, 25 °C, TMS): $\delta = 2.78-2.82$ (m, 2H; OH), 3.39 (s, 3H; OMe), 3.77–4.30 (m, 6H; sugar–CH (H2–6)), 4.73 (s, 1H; sugar–H (H1)), 5.56 (s, 1H; Ph–CH), 7.36–7.39 (m, 3H; *m*,*p*-Ph–H), 7.47–7.51 (m, 2H; *o*-Ph–H); IR (KBr): $\nu = 3650-3000$ (OH), 1020 cm^{-1} (C–O–C); $C_{14}H_{18}O_6$ (282.3): calcd C 59.57, H 6.43; found C 54.89, H 5.94; $C_{14}H_{18}O_6 \cdot 0.25\,CHCl_3$ requires C 54.82, H 5.90.

Methyl-4,6-*O*-benzylidene-*β*-D-glucopyranoside (1b): Compound **1b** was synthesized by means of a method similar to that used for **1a**: yield (1.61 g, 55%) (calculated from methyl-*β*-D-glucopyranoside). M.p. 174–175 °C; ^{1}H NMR (300 MHz, $CDCl_3$, 25 °C, TMS): $\delta = 2.72-2.87$ (q, 2H; OH), 3.39–4.35 (m, 10H; OMe, and sugar–CH (H1–6)), 5.54 (s, 1H; Ph–CH), 7.26–7.39 (m, 3H; *m*,*p*-Ph–H), 7.48–7.51 (m, 2H; *o*-Ph–H); IR (KBr): $\tilde{\nu} = 3700-3200$ (OH), 1030 cm^{-1} (C–O–C); $C_{14}H_{18}O_6$ (282.3): calcd C 59.57, H 6.43; found C 59.36, H 6.49.

Methyl-4,6-*O*-benzylidene-*β*-D-galactopyranoside (2b): Compound **2b** was synthesized by means of a method similar to that used for **2a**: yield (1.02 g, 35%) (calculated from methyl-*β*-D-glucopyranoside). M.p. 180.7–182.9 °C; ^{1}H NMR (300 MHz, $CDCl_3$, 25 °C, TMS): $\delta = 2.55-2.59$ (q, 2H; OH), 3.49–4.38 (m, 10H; OMe, and sugar–CH (H1–6)), 5.56 (s, 1H; Ph–CH), 7.26–7.37 (m, 3H; *m*,*p*-Ph–H), 7.49–7.52 (m, 2H; *o*-Ph–H); IR (KBr): $\tilde{\nu} =$

© WILEY-VCH Verlag GmbH, D-69451 Weinheim, 1999
0947-6539/99/0509-2728 $ 17.50+.50/0 *Chem. Eur. J.* **1999**, *5*, No. 9

3700–3200 (OH), 1030 cm^{-1} (C–O–C); $C_{14}H_{18}O_6$ (282.3): calcd C 59.57, H 6.43; found C 59.23, H 6.48.

Gelation test: A gelator (3.0 mg) was mixed with solvent (0.10 mL) in a septum-capped sample tube and heated in an oil bath until the solid was dissolved. Then, the solution was cooled to 25 °C and left for 1 h. If a stable gel was observed, it was classified as G in Table 1. When the gel was obtained from a solution at a concentration even lower than 1.0 % (wt/vol), it was designated G*.

Gel-sol phase transition temperatures: A test tube containing the gel was inverted in a thermostatted oil bath. The temperature was raised at a rate of 2 °C min^{-1}. Here, the T_{gel} was defined as the temperature at which the gel disappears.

SEM observations: An Hitachi S-900S scanning electron microscope was used for taking the SEM pictures. The thin gel was prepared in a sample tube and frozen in liquid nitrogen. The frozen specimen was dried under vacuum for 3–5 h. The dry sample thus obtained was shielded by gold. The accelerating voltage was 5 kV and the emission current was 10 μA.

Apparatus for spectroscopy measurements: ^{1}H NMR spectra were measured with a Bruker ARX 300 apparatus. IR spectra were obtained in NaCl cells with a Shimazu FT-IR 8100 spectrometer.

Computational methods: Energy minimization was carried out by a MM3 program with AccuModel 1.0 (Microsimulation L. A. Systems Inc.) with a Macintosh computer.

[1] a) K. Hanabusa, K. Okui, T. Koyama, H. Shirai, *J. Chem. Soc. Chem. Commun*. **1992**, 1371, and references therein; b) K. Hanabusa, M. Yamada, M. Kimura, H. Shirai, *Angew. Chem*. **1996**, *108*, 2086; *Angew. Chem. Int. Ed. Engl*. **1996**, *35*, 1949; c) K. Hanabusa, K. Shimura, K. Hirose, M. Kimura, H. Shirai, *Chem. Lett*. **1996**, 885; d) K. Hanabusa, A. Kawakami, M. Kimura, H. Shirai, *Chem. Lett*. **1997**, 191; e) T. Kato, G. Kondo, K. Hanabusa, *Chem. Lett*. **1998**, 193; f) Y. Hishikawa, K. Sada, R. Watanabe, M. Miyata, K. Hanabusa, *Chem. Lett*. **1998**, 795.

[2] E. J. de Vries, R. M. Kellogg, *J. Chem. Soc. Chem. Commun*. **1993**, 238.

[3] M. Takafuki, H. Ihara, C. Hirayama, H. Hachisako, K. Yamada, *Liq. Cryst*. **1995**, *18*, 97.

[4] J.-E. S. Sobna, F. Fages, *Chem. Commun*. **1997**, 327.

[5] a) E. Otsuni, P. Kamaras, R. G. Weiss, *Angew. Chem*. **1996**, *108*, 1423; *Angew. Chem. Int. Ed. Engl*. **1996**, *35*, 1324, and references therein; b) P. Terech, R. G. Weiss, *Chem. Rev*. **1997**, *97*, 3133; c) Y-C. Lin, B. Kachar, R. G. Weiss, *J. Am. Chem. Soc*. **1989**, *111*, 5542; d) I. Furman, R. G. Weiss, *Langmuir* **1993**, *9*, 2084; e) L. Lu, R. G. Weiss, Langmuir **1995**, *11*, 3630; f) L. Lu, R. G. Weiss, *Chem. Commun*. **1996**, 2029.

[6] a) P. Terech, I. Fuman, R. G. Weiss, *J. Phys. Chem*. **1995**, *99*, 9558, and references therein; b) P. Terech, J. J. Allegraud, C. M. Garner, *Langmuir* **1998**, *14*, 3991.

[7] K. Murata, M. Aoki, T. Suzuki, T. Hanada, H. Kawabata, T. Komori, F. Ohseto, K. Ueda, S. Shinkai, *J. Am. Chem. Soc*. **1994**, *116*, 6664, and references therein.

[8] T. D. James, K. Murata, T. Hanada, K. Ueda, S. Shinkai, *Chem. Lett*. **1994**, 273.

[9] S. W. Jeong, K. Murata, S. Shinkai, *Supramol. Sci*. **1996**, *3*, 83.

[10] T. Brotin, R. Utermolen, F. Fagles, H. Bouas-Laurent, J.-P. Desvergne, *J. Chem. Soc. Chem. Commun*. **1991**, 416.

[11] a) J. van Esch, S. de Feyter, R. M. Kellogg, F. de Schryver, B. L. Feringa, *Chem. Eur. J*. **1997**, *3*, 1238; b) R. Oda, I. Huc, S. J. Candau, *Angew. Chem*. **1998**, *110*, 2835; *Angew. Chem. Int. Ed*. **1998**, *37*, 2689.

[12] S. Yamasaki, H. Tsutsumi, *Bull. Chem. Soc. Jpn*. **1996**, *69*, 561, and references therein.

[13] K. Yoza, Y. Ono, K. Yoshihara, T. Akao, H. Shinmori, M. Takeuchi, S. Shinkai, D. N. Reinhoudt, *Chem. Commun*. **1998**, 907.

[14] M. Svaan, T. Anthonsen, *Acta. Chem. Scand. Ser. B* **1986**, *40*, 119.

[15] The following solvents were also tested: *m*-cresol, tetrahydrofuran, dioxane, *N*,*N*-dimethylacetamide, *N*,*N*-dimethylformamide, dimethyl sulfoxide, 1-methyl-2-pyrrolidone, methanol, benzyl alcohol, acetic acid, *n*-propylamine, diethylamine, aniline, pyridine, and 2,2,2-trifluoroethanol, but all the five gelators were too soluble in these solvents and gels were not formed.

[16] The same idea was also proposed by Weiss et al. on the basis of the spectroscopic data in Ref. [5] and R. Mukkamala, R. G. Weiss, *J. Chem. Soc. Chem. Commun*. **1995**, 375.

[17] A similar correlation between the ΔH and the gelator solubility was found in a related system. See N. Amanokura, K. Yoza, H. Shinmori, S. Shinkai, D. N. Reinhoudt, *J. Chem. Soc. Perkin Trans. 2* **1998**, 2585.

[18] In a preliminary communication,[13] the explanation of this figure (plots of *R* against gelator concentration) is partially confused.

[19] M. Aoki, K. Nakashima, H. Kawabata, S. Tsutsui, S. Shinkai, *J. Chem. Soc. Perkin Trans. 2* **1993**, 347.

[20] N. Inamoto, *Hamme Rule*, Maruzen, Tokyo, **1983**, p. 90.

[21] K. Araki, K. Iwamoto, S. Shinkai, T. Matsuda, *Bull. Chem. Soc. Jpn*. **1990**, *63*, 3480.

[22] For the preparation of dry samples for SEM observations, see ref. [7] and S. W. Jeong, S. Shinkai, *Nanotechnology* **1997**, *8*, 179.

[23] We estimated the heat of formation for C1–**2a** and 1C–**2a** by MOPAC PM3. However, the energy difference was not significant enough to alter their relative stability (–900 and –875 kJ mol^{-1} respectively).

Received: December 21, 1998 [F1501]